Int J CARS (2011) 6:201–208
DOI 10.1007/s11548-010-0500-1

ORIGINAL ARTICLE

Validation and prediction of traditional Chinese physical operation on spinal disease using multiple deformation models

Lei Pan · Xubo Yang · Lixu Gu · Wenlong Lu · Min Fang

Received: 11 January 2010 / Accepted: 1 June 2010 / Published online: 24 June 2010

Abstract
Purpose Traditional Chinese medical massage is a physical manipulation that achieves satisfactory results on spinal diseases, according to its advocates. However, the method relies on an expert's experience. Accurate analysis and simulation of massage are essential for validation of traditional Chinese physical treatment. The objective of this study is to provide analysis and simulation that can reproducibly verify and predict treatment efficacy.
Methods An improved physical multi-deformation model for simulating human cervical spine is proposed. First, the human spine, which includes muscle, vertebrae and inter-vertebral disks, are segmented and reconstructed from clinical CT and MR images. Homogeneous landmark registration is employed to align the spine models before and after the massage manipulation. Central line mass spring and contact FEM deformation models are used to individually evaluate spinal anatomy variations. The response of the human spine during the massage process is simulated based on specific clinical cases.
Results Ten sets of patient data, including muscle–force relationships, displacement of vertebrae, strain and stress distribution on inter-vertebral disks were collected, including the pre-operation, post-operation and the 3-month follow-up. The simulation results demonstrate that traditional Chinese massage could significantly affect and treat most mild spinal disease.
Conclusion A new method that simulates a traditional Chinese medical massage operation on the human spine may be a useful tool to scientifically validate and predict treatment efficacy.

Keywords Multiple deformation models · Contact FEM · Traditional Chinese massage · Spinal disease

L. Pan · X. Yang · W. Lu
School of Software, Shanghai Jiao Tong University, Shanghai, China

L. Gu (✉)
Med-X Research Institute, Shanghai Jiao Tong University, Shanghai, China
e-mail: gulixu@sjtu.edu.cn; gu-lx@cs.sjtu.edu.cn

M. Fang
Shanghai Yuanyang Hospital, Shanghai, China

Introduction and related work

Currently, spinal diseases become common chronic refractory diseases in China. The prevalence of cervical and lumbar spinal diseases increases in recent years, and the morbidity is among the highest rates. More than half of the Chinese people aged over 50 have varying degrees of symptoms in cervical spine. More consistent points of view in the medical profession area still believe that at least 90% of the spinal diseases, of which morbidity were mainly caused by the pathological changes on inter-vertebral disks, should conduct non-surgical therapy as the first choice. Traditional Chinese medical (TCM) massage, which was invented and developed in ancient China, can be considered as the primary means of intervention. Though the application to the treatment of spinal disease has achieved satisfactory results, the parameters–effect relationship and the criterion of evaluation are still to be standardized. Liu et al. [11] introduced a standardized representation model and case application of TCM massage therblig. Cherkin et al. [4] provided a review and summary of the available evidence about the effectiveness of the most popular complementary and alternative medical therapies, including TCM massage.

However, more research and experiments need to be done on a large number of clinic cases to scientifically evaluate and illustrate the effect of traditional Chinese medical massage. The massage operation, which includes three series of TCM therblig and lasts 10 days, 2 h each day, is conducted by the physicians of Shanghai University of TCM. We refer the term "massage operation" to the whole process of this treatment in this paper. Just like many other virtual surgery systems, the computer techniques were employed to simulate the response of the whole spine during the massage operation and calculate the stress distribution, which is difficult to measure, on both muscles and inter-vertebral disks. Once the research gains a large amount of satisfactory simulation data, the physicians can give accurate prediction before conducting the massage operation on patients based on the calculated results. Moreover, the simulation can provide junior physicians with practical and standardized therblig training.

As the development of the techniques in computer graphics and the research on image guided virtual surgery and therapy, numbers of new methods were proposed to simulate different traditional surgery and therapy. Contact FEM provides an engineering method for medical simulations [13]. Hirota et al. [8] proposed a limited frictionless algorithm for the contact problem and applied this algorithm to the human body. Rohlmann et al. [15] studied the effect of an artificial disk on lumbar spine biomechanics using a probabilistic finite element method. The development of GPU brought a revolution in series of conventional image processing and computer graphics algorithms. Mass spring systems [7] and fast FEM [10] can be achieved and accelerated on the GPUs. This study was encouraged by the mentioned progress and tries to provide accurate and reliable analysis and simulation of the TCM massage operation to the physicians and therefore help them to validate and predict the operation.

In the rest of the paper, novel multiple deformation models for the whole spine is proposed in "Methods" section. The mathematical and physical principle of the simplified contact FEM is introduced. GPU-aided computation, basic process for simulating the TCM massage operation in our system and related information are also mentioned. In "Experimental results" section, the background of the experiments and results of the massage operation simulation are shown. Three sets of clinic cases are compared and studied. The shift of the vertebrae, the deformation of the muscle, the strain and stress of the inter-vertebral disks are illustrated. At last, we summarized our research on computer-aided TCM spinal massage operation simulation. In the "Conclusion" section, TCM massage operation is considered as an effective treatment on some mild spinal disease. Our methods are feasible and accurate enough to provide a reliable tool for the physicians to validate and predict the efficacy of operation.

Methods

Considering the specific anatomic structure of human spine and the characters of the TCM massage operation, multiple spine deformation models, which include central line mass spring model and simplified contact FEM model, are proposed. Here, we pay more attention on the contact FEM model since it is improved and simplified to simulate the inter-vertebral disks, which are the most interest and important parts of the spine disease. We implemented the simulation of the whole operation process by simply exerting continuous external forces on the specific locations. And then the response of the human spine is calculated with or without the help of GPU parallel computation.

Multiple spine models

In the image-preprocessing stage, the patients were scanned by CT and MR device. We segment and reconstruct the vertebrae from these CT images. Meanwhile, we segment inter-vertebral disks, trapezius and latissimus dorsi, including longitudinal and supraspinous ligaments from MR images and reconstruct them as deformable soft issues (Fig. 1).

The structures of human spine are best resources for multiple deformable methods modeling. Lin and Sucato [9] used the 3D Bezier Curve to model the simplified 3D human spine for analyzing and classifying the scoliotic deformity. Vertebra is modeled as a rigid body, and the inter-vertebral disks are modeled as springs by Furukawa et al. [5]. Since trapezius and latissimus dorsi are directly affected by the external force from the physician who conducts the medical massage operation, we describe and record the operation process in several professional parameters on these muscles according to the requirements that the hospital provided. Based on the strip feature of trapezius and latissimus dorsi, customized Central Line mass spring model is employed. We assume that traditional Chinese approach of medical massage operation would not have any effect on vertebrae's volume, shape, density and relative position of internal vertices. Since the vertebrae are modeled as rigid bodies, the influence on vertebrae after the operation can be considered as rigid transform. Therefore, the information of vertebral translation and rotation is obtained by conducting CT–CT rigid registration. Moreover, inter-vertebral disks play quite an important role in spinal disease that presses the spinal cord causing the symptom and pain. To emphasize every fine deformation and accurate stress distribution, non-friction contact FEM deformable model, which is the most accurate deformation analysis method under complex environments and conditions, is employed in our research. In this paper, we will mainly discuss the methods of modeling the real human spine with multiple deformable models, computing the stress and

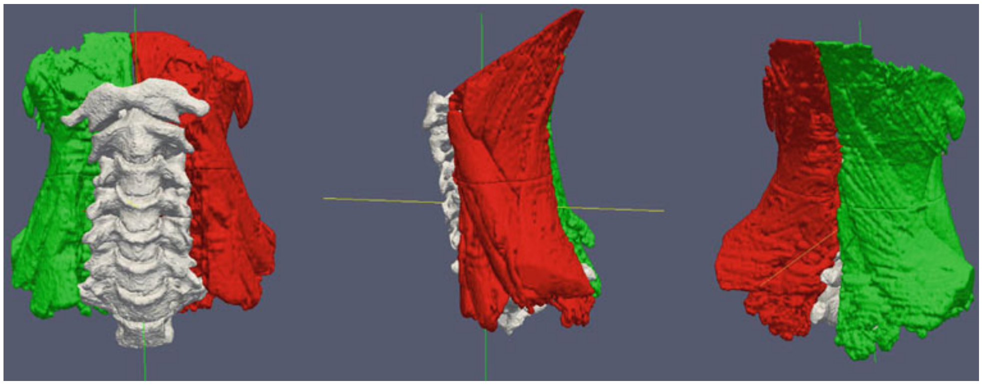

Fig. 1 Reconstruction of trapeziuses, latissimus dorsi and cervical vertebrae. *Left* and *right* trapeziuses, which are directly and respectively under the pressure from the physician, are labeled with *red* and *green* colors. The cervical vertebrae are labeled with *white* color

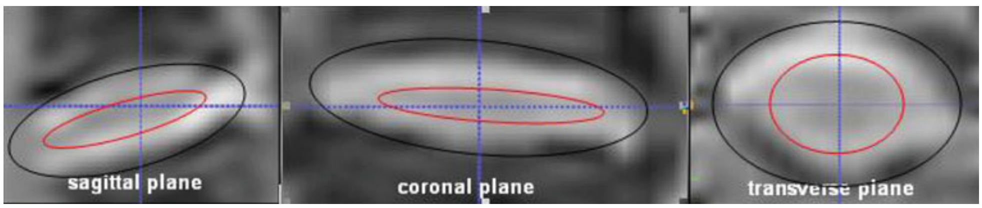

Fig. 2 Annulus–nucleus structures of an inter-vertebral disk in MR image. The inter-vertebral disk is labeled with a *black circle*. The annulus–nucleus is labeled with a *red circle*

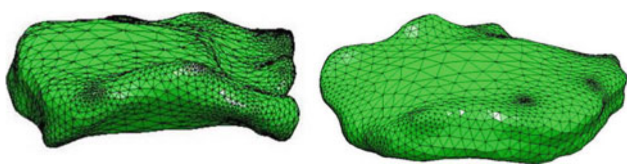

Fig. 3 Reconstruction of inter-vertebral disks from MR image

strain of the models and simulating the results of traditional Chinese medical massage operation.

Inter-vertebral disks, which consist of annulus and nucleus, are dual-material structures. Both annulus and nucleus of the inter-vertebral disks can be segmented from high-quality MR images (Fig. 2). High-quality tetrahedron mesh of both annulus and nucleus are precisely built and optimized (Fig. 3) by mesh reconstruction program [12]. Although the contact FEM is well developed for engineering analysis and competent for such intricate situation, the heavy computation load and large scale of memory occupancy are practical problems in our research. According to the real properties and characters that human spine behaves during the operation, we propose a simplified form of constrained variational principle when solving contact FEM equation.

Methods of simulation implementation

In the massage operation stage, the external forces exerted by the physicians were located on the deformation mesh models of cervical muscles. During the operation, the deformation on cervical muscles caused by continuously exerted forces is simply simulated and calculated by the conventional central line mass spring model. The central lines in both latissimus dorsi and trapezius are separately moved with the adjusted stiffness coefficient of the mass spring. Based on the direction and the size of the exerted force, the displacements caused by the deformed muscle were directly passed to the vertebrae (Fig. 4). The strain and stress of the inter-vertebral disks were calculated based on these displacements and boundary conditions. When the exerted forces were removed, the muscle and vertebrae have the tendency to rebound. The patients were scanned by CT and MR devices for the second time, and the strain and stress of the disks were calculated again right after the operation. We compared the previous and post-operation images to calculate and validate the results. At last, 3 months after the whole process of the massage operation, the patients were scanned again for the third time. Another calculation is conducted in order to review the long-term effects.

Contact FEM

External force conducted by the physician takes place on trapezius, which is simulated by central line mass spring with the pre-adjusted stiffness parameter. The displacements directly pass to the vertebra where supraspinous ligament attaches. We update the boundary condition and contact condition of inter-vertebral disks based on the surface

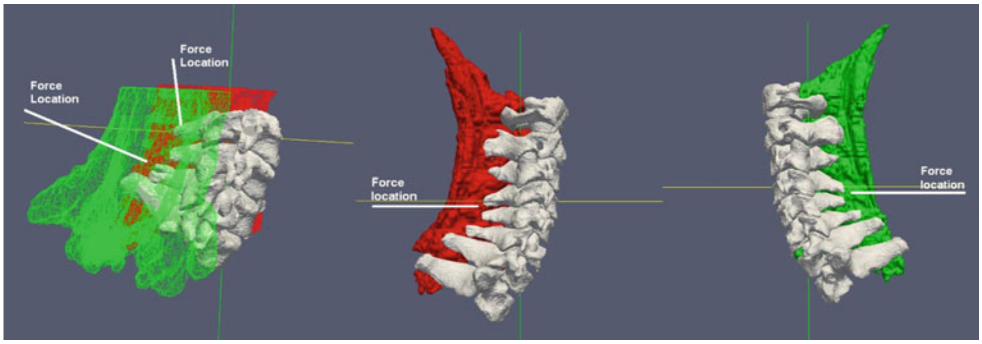

Fig. 4 External forces are located on trapezius and directly passed to the vertebra through mass spring muscles. The physicians were asked to record the direction and the size of their exerted forces

vertices in iteration. Severe non-linear constrain on the contact surfaces is controlled by contact vertices pairs. Since the surfaces of vertebrae and inter-vertebral disks are adhesive, so are the surfaces of inner annulus and nucleus, friction and separate status between vertebrae and annuluses are ignored. (However, in conventional contact FEM problem, several complex conditions are considered.) We assume that there is no relative sliding; the contact surfaces area and the contact vertices pairs remain the same during entire operation process. Suppose one of the contact vertices pairs are $\boldsymbol{P}$ on contactor $\boldsymbol{A}$, and $\boldsymbol{Q}$ on target $\boldsymbol{B}$, the non-penetration conditions on time $\boldsymbol{t}$ are considered as

$$^{t}g_N = g\left({}^{t}x_P^A, t\right) = \left({}^{t}x_P^A - {}^{t}x_Q^B\right) \cdot {}^{t}n^B \equiv 0 \tag{1}$$

$$u^A - u^B \equiv 0 \tag{2}$$

where $^{\boldsymbol{t}}\boldsymbol{g}_{\boldsymbol{N}}$ refers to the minimum distance between vertices $\boldsymbol{P}$ and $\boldsymbol{Q}$. While there are relative movements on vertices, their coordinate $\boldsymbol{x}_{\boldsymbol{P}}^{\boldsymbol{A}}, \boldsymbol{x}_{\boldsymbol{Q}}^{\boldsymbol{B}}$ and the displacement $\boldsymbol{u}^{\boldsymbol{A}}, \boldsymbol{u}^{\boldsymbol{B}}$ stay the same.

Contact forces that along the normal direction can be both pressure and tension. Both contactor $\boldsymbol{A}$ and target $\boldsymbol{B}$ are two independent bodies to be solved. Besides the conventional FEM minimum potential energy formula, we imported severe boundary non-linear restriction:

$$\min \Pi(U) = \frac{1}{2}U^T KU - U^T F$$
$$g \geq 0 \tag{3}$$

where the potential energy π of the deformed object is a function of parameter $\boldsymbol{U}$, which is the displacement field of the nodes. The parameter $\boldsymbol{K}$ refers to the stiffness matrix of the current object. The parameter $\boldsymbol{F}$ refers to the external load of the system, and $\boldsymbol{g}$ is still the minimum distance. According to the principle of virtual displacement, we import the virtual work $^{\boldsymbol{t}}\boldsymbol{W}_{\boldsymbol{c}}$ on time $\boldsymbol{t}$ of the contact forces on contact surfaces. The parameter $^{\boldsymbol{t}}\boldsymbol{W}_{\boldsymbol{L}}$ is the virtual work of external load on time $\boldsymbol{t}$,$^{\boldsymbol{t}}$ $\boldsymbol{W}_{\boldsymbol{I}}$ is the virtual work of inertial forces, which is a constant 0 in our method.

$$\int_{^{t}V} {}^{t}\tau \cdot \delta_t e \cdot {}^{t}dV - {}^{t}W_L - {}^{t}W_I - {}^{t}W_C = 0 \tag{4}$$

$$^{t}W_c = \int_{^{t}S^A} {}^{t}F^A \cdot \delta u^A \cdot {}^{t}dS + \int_{^{t}S^B} {}^{t}F^B \cdot \delta u^B \cdot dS \tag{5}$$

where $^{\mathrm{t}}\boldsymbol{\tau}$ is the Euler stress on time $\boldsymbol{t}$. $\boldsymbol{\delta}_{\mathrm{t}}\boldsymbol{e}$ is the corresponding variation of the infinitesimal strain $_{\mathrm{t}}\boldsymbol{e}$. The integral term $\int_{\mathrm{v}}^{\mathrm{t}} \boldsymbol{\tau} \cdot \boldsymbol{\delta}_{\mathrm{t}}\boldsymbol{e} \cdot^{\mathrm{t}} dV$ is the virtual work of the virtual displacement on time $\boldsymbol{t}$, which equals the virtual work of the external load $\boldsymbol{W}_{\boldsymbol{L}}$, $\boldsymbol{W}_{\boldsymbol{I}}$ and $\boldsymbol{W}_{\boldsymbol{C}}$. The virtual work of the contact force $\boldsymbol{W}_{\boldsymbol{C}}$ on time $\boldsymbol{t}$ includes two parts. $^{\boldsymbol{t}}\boldsymbol{S}^{\boldsymbol{A}}$ and $^{\boldsymbol{t}}\boldsymbol{S}^{\boldsymbol{B}}$ refer to the contact surfaces on contact objects $\boldsymbol{A}$ and $\boldsymbol{B}$. $\boldsymbol{\delta u}^{\boldsymbol{A}}$ and $\boldsymbol{\delta u}^{\boldsymbol{B}}$ are the variation of the displacements $\boldsymbol{u}$ on objects $\boldsymbol{A}$ and $\boldsymbol{B}$.

Using Lagrange multiplier method, we import Lagrange multiplier $\boldsymbol{\lambda}$ and define the contact constrain condition in another form $\boldsymbol{\pi}_{\mathbf{c}} = \boldsymbol{g}^{\mathbf{T}}\boldsymbol{\lambda}$. Finally, the minimum problem without the restriction $\boldsymbol{g} \geq 0$ after importing Lagrange multiplier is presented as:

$$\min \Pi\,(U, \lambda) = \frac{1}{2}U^T KU - U^T F + g^T \lambda \tag{6}$$

Taylor extension for the contact restriction condition $\boldsymbol{g}$ is a function of displacement $\boldsymbol{U}$. ($\boldsymbol{g}_{\boldsymbol{0}}$ is the initial distance of the contact vertices pair):

$$g(U) \approx g_0 + \frac{\partial g}{\partial U}U = g_0 + GU \tag{7}$$

The final system equation in **total Lagrange formulation** to be solved with multiplier $\boldsymbol{\lambda}$ is:

$$M^t\upsilon + \begin{bmatrix} {}_0^tK_L + {}_0^tK_{NL} & K_\lambda \\ K_\lambda^T & 0 \end{bmatrix} \begin{bmatrix} u \\ {}^t\lambda \end{bmatrix} = \begin{bmatrix} {}^tQ - {}_0^tF \\ -{}^tg \end{bmatrix} \tag{8}$$

or rewritten in a simpler form $\begin{bmatrix} K & G^T \\ G & 0 \end{bmatrix} \begin{bmatrix} U \\ \lambda \end{bmatrix} = \begin{bmatrix} F \\ -g_0 \end{bmatrix}$. The current displacements $\boldsymbol{U}$ on time $\boldsymbol{t}$ are solved in this equation. The stiffness matrix and other related functions are updated before the next iteration.

GPU computation

In order to solve the Eq. (8) with larger scale in high efficiency, GPU and related solver are employed. Bolz et al. [1] introduced sparse matrix solvers on the GPU. Two basic, broadly useful, computational kernels: a sparse matrix conjugate gradient solver and a regular-grid multi-grid solver were implemented. By using these methods, the scales of matrices were reduced, Ill-conditioned matrices with 0 matrix diagonal elements were successfully solved to the maximum extent. Non-linear part of the materials and geometry of FEM were organized and solved in total Lagrange formulation by incremental analysis. In our research, the incremental iteration is implemented by CUDA (Fig. 5).

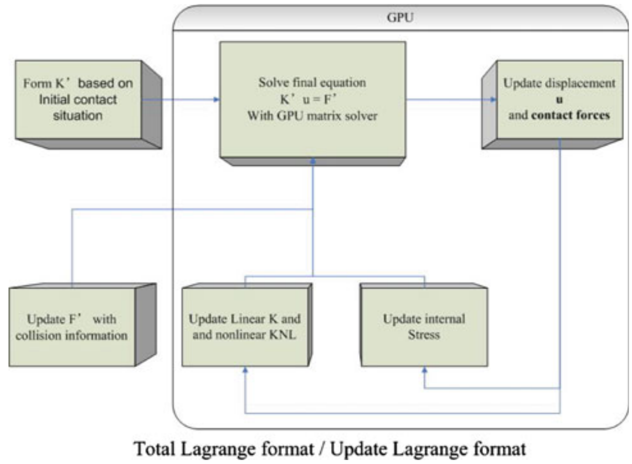

Fig. 5 The procedure of the iterative contact FEM deformation computation

Experimental results

The complete design and process of our simulation experiments are illustrated in Fig. 6. In order to accurately simulate the TCM massage operation and validate the efficacy of the treatment, we acquire both MR and CT images covering 8 sections (L1-L8, begin from the first vertebra under the cranial cavity) of cervical vertebra from 10 patients (P1-P10), who suffered varying degrees of symptoms in cervical spine, from Shanghai Longhua Hospital. There are three sets of MR and CT data for each patient, including pre-operation, post-operation and 3-month post-operative review. The dimension of the image is 512 * 512 * 695 with the voxel spacing of 0.4, 0.4 and 0.3 mm. In order to verify the operation results on shifted vertebrae, segmentation, reconstruction and semi-automatic registration are employed to detect the position deference. Since the segmentation and registration results may directly affect the final results, several methods were used for both CT and MR to avoid errors. We segmented the vertebrae and inter-vertebral disks in MRI and then check the surface of both vertebrae and disks in CT. Special marks

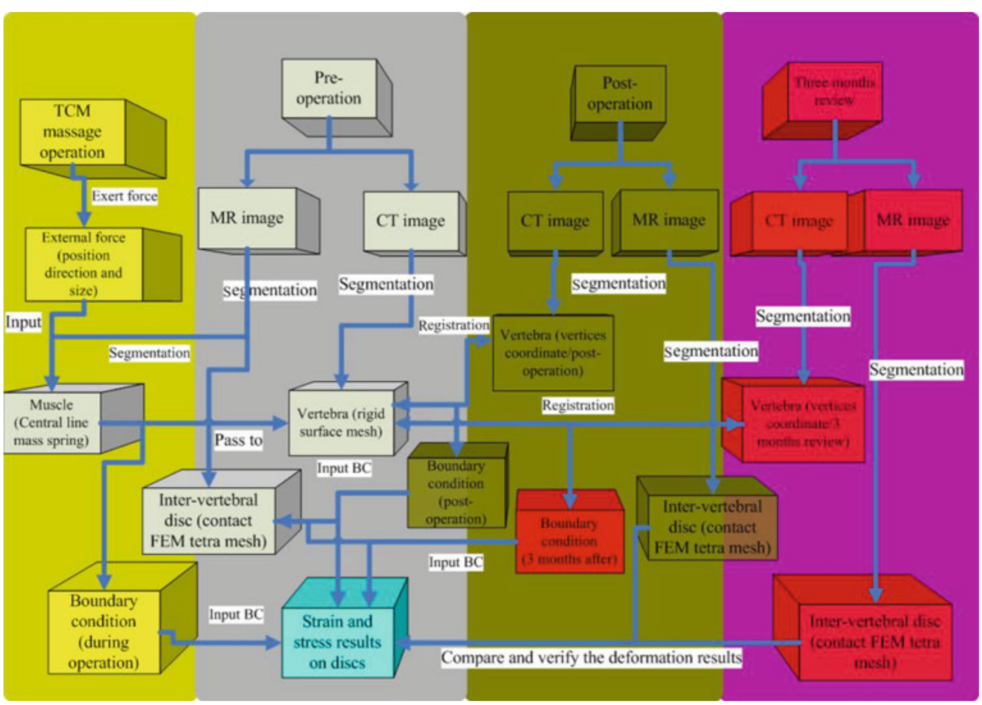

Fig. 6 The design and the process of the TCM massage operation simulation experiment. Results gained from different stages are labeled with the different colors. "Pre-operation" stage is *gray*. "Post-operation" stage is olive *green*. "Three-month review" stage is *red*." The static operation stage" is *yellow*

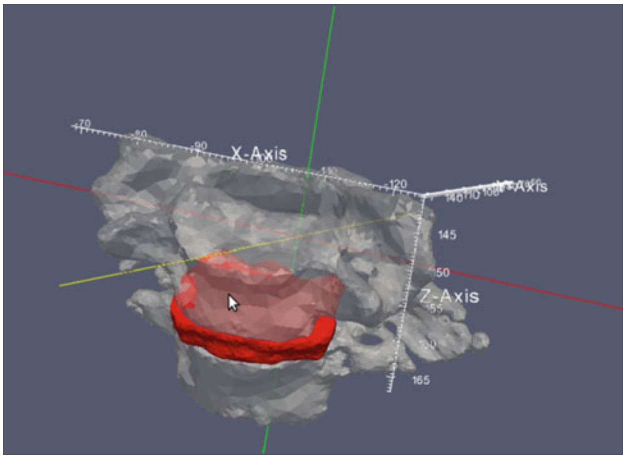

Fig. 7 Structure of cervical vertebrae and inter-vertebral disk after registration

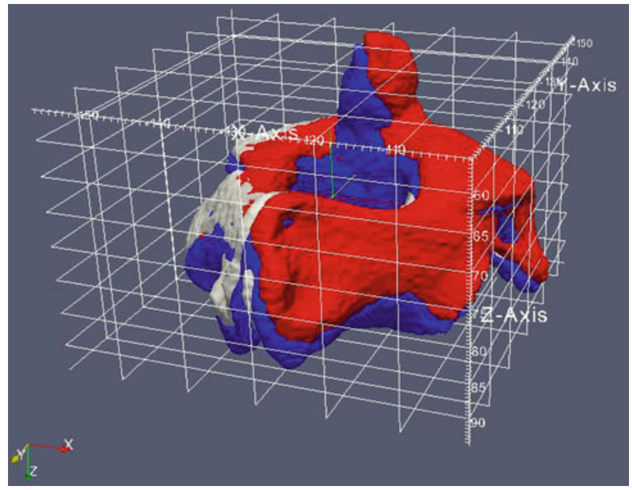

Fig. 8 The base coordinate system used for the calculation of rotation and translation. All related work, including registration, external force localization, is based on this system from original medical image

were located in both MR and CT devices for more accurate semi-automatic rigid landmark registration. Patients who were taken MR and CT images before and after the operation were required and instructed to lie on the same position with the same gesture. It can be considered that there is no big error, which may essentially affect the simulation result, caused by segmentation and registration in our ten experimental cases (Fig. 7).

In Table 1, we recorded, calculated and compared the transform in both rotation and translation according to the central point of the mesh data. The translation and rotation of each vertebra are based on the original coordinate system of the CT images (Fig. 8). We assume that the vertebrae of the patients do not change during the whole observation process. We found out that most patients who suffered from spinal disease had the similar causes. One or two of their vertebrae were most shifted and rotated in the same direction. Obvious corrections on the vertebrae caused by the operation were found between pre-operation and post-operation. The final statuses of the three stages were labeled with different colors (Fig. 9). However, it is also found in Table 1 that the situation rebounded to varying degrees after 3 months.

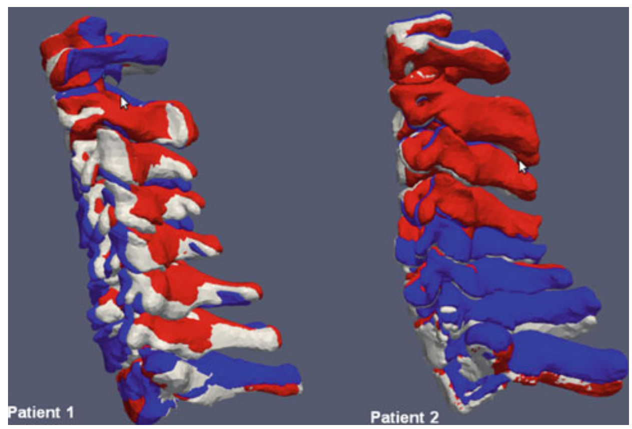

Fig. 9 Comparisons of cervical vertebrae L1-L8 of two patients (P1 and P2) in three stages with different color labels. *White color* refers to status before massage operation (Stage 1). *Red color* refers to the status just after the massage operation (Stage 2), and *blue color* refers to the status 3 months after massage operation (Stage 3)

After the whole spinal models are built and aligned, external force could also be exerted based on the coordinate system in Fig. 8. The therblig conducted by the physicians is unique to different patients. Therefore, we can assume that the size

Table 1 Traditional Chinese medical massage operation effects on vertebrae

Compared transformed vertebrae in 10 patients	Average rotation (angles to the central axis in degree)			Average translation (displacement of the central point in mm)		
	x	*y*	*z*	*x*	*y*	*z*
Pre-operation to post-operation	±3.02	±0.98	±0.14	±1.77	±0.84	±0.21
Pre-operation to 3-month post-operative review	±2.83	±0.95	±0.15	±1.56	±0.82	±0.21

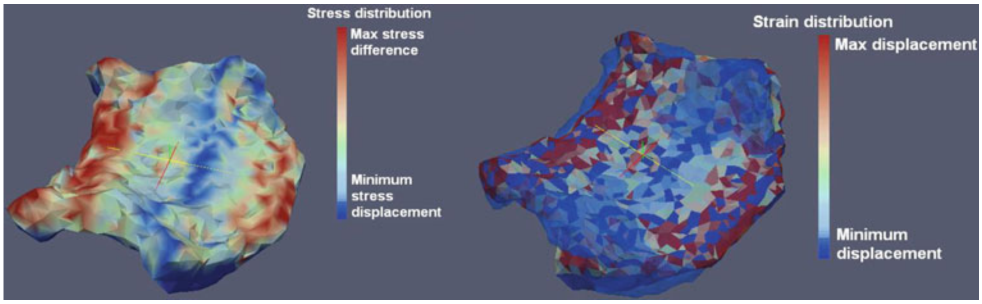

Fig. 10 The example of the final node stress and strain distribution result after contact FEM computation. In the *left* figure, node stresses are expressed as absolute values in all directions. The nodes with the *blue* color mean that there is no stress change after the massage operation compared to the status before the massage operation. In the *right* figure, the strain distribution on surface is illustrated in the form of displacement. The half transparent *blue* mesh is the original status before the massage operation. This figure illustrated that both front and *back* sides (in *y* axis) of the inter-vertebral disk endure most stress changes and have the maximum displacement

Table 2 Comparison of calculated results in strain and stress

Compared data	Strain (compare calculated results to actual images)	Stress (compare stress distributions before and after the operation)
Post-operation	Average ±0.16 mm	Suffer average ±1.244 N on all nodes
3-month post-operative review	Average ±0.19 mm	Suffer average ±0.81 N on all nodes

and the direction of the exerted force are continuous and stable on the muscle. We call this process the "Static operation stage". In this way, the response of the spine under the pressure is simulated. The physicians could clearly observe the effects of the specific therblig in the anatomic view. However, this effect in the "Static operation stage" could not be accurately examined like the results in "post-operation stage" and "Three-month review stage" because the human spines rebound right after the external force is removed.

Distribution of strain and stress on inter-vertebral disk before and after the operation is the most important result that may cause spinal stenosis. We consider the accuracy of the final FEM computational results on both strain and stress. In our experiments, the value of Young's modulus is approximately 15 kPa for the annulus and 3 kPa for nucleus. The value of Poisson ratio is 0.3. The initial boundary conditions for the inter-vertebral disks include the contacted surfaces of their upper and lower vertebrae, the inner surface of the annulus and the outer surface of the nucleus. The contact vertices pairs on both contactor and target are overlapped when we built the tetrahedron mesh. And we assume that they never separate during the operation. The coordinate of the contact vertices pairs are calculated and updated in iteration, and severe non-linear constrain is imported.

The strain and deformation results were simply verified by comparing the calculated mesh to the actual MR and CT images after the operation (Fig. 10). We record the average absolute displacements of the surface vertices in Table 2. However, it is more difficult to find a proper method and measurement to evaluate the stress results. In order to indicate the medical effects, we assume that the stress distribution on inter-vertebral disk before the massage operation is uniform. After the massage operation, the stress distribution changed on inter-vertebral disks and was labeled as different colors by values. Red colors indicated the areas were with most pressure change and had the trends of extrusion or shrinkage. As shown in Table 2, the inter-vertebral disks receive more stress compared to the original status, which forced the disks to deform back to the healthy shape and condition, when just completed a period of massage operation than 3 months after the operation.

In Table 3, we listed the computation costs in different conditions. Both of our CPU and GPU methods are stable when dealing with the inter-vertebral disk mesh with single structure and homogeneous material. However, the computation became unstable and unreliable when the disk mesh is more complex. In the experiment on disk mesh of small scale (including annulus with 3,650 vertices and nucleus with 960 vertices), it takes about 181 s to complete the equation solving iteration of both parts and update or adjust the stiffness matrices. On the other hand, when GPU was employed to aid the process in parallel way, it takes about 20 s. Some of the deformed vertices on annulus and nucleus may overlap during the iteration since some boundary condition cannot be properly parallelized.

We examine the contact FEM computation in both CPU version and GPU-implemented version. All four sets of inter-vertebral disk mesh data were computed in Pentium® Dual-Core E5200 and 4.00 GB of RAM. The Graphic hardware is NVIDIA 8800.

Table 3 FEM computation results on different inter-vertebral disks data

Inter-vertebral disk data type	Single structure with homogeneous materials		Annulus–nucleus structure with two materials in adjusted parameters	
Total vertices number	3,877	9,864	3,650 + 960	13,270 + 2,435
CPU computation	6,871 ms	38,575 ms	181 s	Not convergence
GPU-aided computation	4,733 ms	9,645 ms	20,687 ms (failed)	Not convergence

Conclusion

According to the results of our study, traditional Chinese medical massage operation achieved good results on mild symptoms of a number of spinal disease cases. It is an acceptable intervention and choice for patients who are in their early stage of spinal disease and unable or unwilling to receive conventional surgery treatment.

In the study, human spine structures are well simulated and calculated by multi-deformable models. Customized central line mass spring model simulates the muscles and ligaments with high efficiency and acceptable accuracy. Displacement is calculated and external force is passed to the vertebra that suffers. Here, we focused on the adjusted contact FEM model, which simplifies the contact constrain condition according to the actual situation and properties of human inter-vertebral disks. Heavy computation load is reduced. Although the computation on large data with complex structure is unstable, it is still possible to provide satisfactory data of displacement, rotation, stress and strain distribution to physicians. These data are acceptable to the physicians and help them to validate and predict the results of massage operation.

As the future works, experiments on more irregular cases need to be further investigated. Large amounts of data on complex mesh need to be recorded and analyzed to provide convincible evidences and prediction for both physicians and patients. The existing error risk of the proposed approach could also be improved by the clinical trial. In the current stage, physicians could not use our result as the only evidence but an aspect of reference.

Acknowledgments The authors are grateful to Shanghai University of TCM and Shanghai Longhua hospital for providing large amounts of clinical cervical spine CT and MR images. The research is partially supported by the Natural Science Foundation of China with Grant No. 60872103, National High Technology Research and Development Program of China with No. 2007AA01Z312 and the 973 National Research Program with No. 2007CB512700-1.

References

1. Bolz J, Farmer I, Grinspun E, Schroder P (2003) Sparse matrix solvers on the GPU: conjugate gradients and multigrid. In: International conference on computer graphics and interactive techniques, ACM SIGGRAPH 2003 papers, p 917–924
2. Chai J, Sun J, Tang Z (2001) Hybrid FEM for deformation of soft tissues in surgery simulation. International workshop on medical imaging and augmented reality (MIAR '01), 2001, p 298
3. Chaichanasiri E, Nanakorn P, Tharanon W, Vander Sloten J (2009) A finite element study of the effect of contact forces between an implant-retained crown and its adjacent teeth on bone stresses. J Mech 25(4):441–450
4. Cherkin DC, Eisenberg D, Sherman KJ, Barlow W, Kaptchuk TJ, Street J, Deyo RA (2001) Randomized trial comparing traditional Chinese medical acupuncture, therapeutic massage, and self-care education for chronic low back pain. Arch Intern Med 161:1081–1088
5. Furukawa D, Kitasaka T, Mori K, Suenaga Y, Mase K, Takahashi T (2004) Spine posture estimation method from human images using 3D spine model computation of the rough approximation of the physical forces working on vertebral bodies. In: Proceedings of the 17th international conference on pattern recognition, 2004. ICPR 2004, 23–26 Aug 2004, vol 3, p 322–325
6. Georgii J, Echtler F, Westermann R (2005) Interactive simulation of deformable bodies on GPUs. In: Simulation and visualisation 2005, p 247–258
7. Georgii J, Westermann R (2005) Mass-spring systems on the GPU. In: Simulation modelling practice and theory, Vol 13, Issue 8, November 2005, p 693–702
8. Hirota G, Fisher S, State A (2003) An improved finite-element contact model for anatomical simulations. Vis Comput 2003(19):291–309
9. Lin H, Sucato D (2004) Identification of lenke spine deformity classification by simplified 3D spine model. Engineering in medicine and biology society, 2004. IEMBS '04. 26th Annual international conference of the IEEE 2:3144–3146
10. Liu Y, Jiao S, Wu W, De S (2008) GPU accelerated fast FEM deformation simulation. Circuits and systems, APCCAS 2008, IEEE Asia Pac Conf p 606–609, Nov 30 2008–Dec 3 2008
11. Liu C, Jiang Z-H, Liu Y-L (2009) Standardized representation model and case application of TCM massage therblig. Comput Eng 35(11):20–22,25
12. Lv S, Gu L, Pan L (2009) Delaunay mesh reconstruction from 3D medical images based on centroidal voronoi tessellations. In: Proceedings of the international conference on computational intelligence and software engineering, p 1–4
13. Nealen A, Müller M, Keiser R, Boxerman E, Carlson M (2005) Physically based deformable models in computer graphics. In: Eurographics 2005
14. Ranzuglia G, Cignoni P, Ganovelli F, Scopigno R (2006) Implementing mesh-based approaches for deformable objects on GPU. In: Fourth eurographicsItalian chapter, eurographics association, p 213–218, Feb 2006
15. Rohlmann A, Mann A, Zander T, Bergmann G (2009) Effect of an artificial disc on lumbar spine biomechanics: a probabilistic finite element study. Eur Spine J 18(1):89–97